



# Salp Swarm Algorithm Tuned Control Scheme for Mitigating Frequency Deviations in Hybrid Power System and Comparative Analysis

Shilpam Malik<sup>1</sup> and Sathans Suhag<sup>2</sup>

<sup>1,2</sup>Electrical Engineering Department, National Institute of Technology, Kurukshetra, Haryana, India

Received 05 Mar.2020, Revised 29 Mar. 2021, Accepted 03 Apr. 2021, Published 02 May. 2021

**Abstract:** In this paper, a salp swarm algorithm (SSA) tuned fractional order fuzzy proportional integral derivative (FOFPID) control scheme is designed and implemented for mitigation of frequency deviations under varying operating conditions in a hybrid power system (HPS) due to load variations and variable power output of renewable energy sources (RESs). The essence of the paper is in the use of SSA for optimal tuning of the controller. The performance of SSA tuned FOFPID controller is compared against other controllers, tuned using SSA. The supremacy of SSA is also established against the other four evolutionary optimization algorithms. The novel control scheme is evaluated with and without different energy storage systems (ESSs) and diesel engine generator (DEG) besides parametric variations of one of the ESSs. The results are indicative of the proposed control scheme being very efficient and effective. MATLAB® is the platform used for running the simulations.

**Keywords:** Hybrid Power System, Salp Swarm Algorithm, Renewable Energy Sources, FOFPID.

## 1. INTRODUCTION

With increasing population the electric load demand is also increasing drastically. To cater to this increasing demand, more power is being generated major portion of which still comes from conventional sources although the power system is witnessing a rising trend of penetration of RESs, in particular wind and solar energy, necessitated by the adverse effects of the conventional sources on environment. However, with RESs there are associated challenges due to the weather uncertainties. The unpredictable variations in load coupled with the intermittency of RESs leads to constant mismatch in generation and consumption of power in a HPS. This imbalance leads to the frequency deviation [1] which is required to be minimized to ensure smooth and stable operation of HPS. In such situations, it is the ESSs that can come to the rescue and restore the balance by injecting power into the HPS when it is in deficit of power and extracting power from the HPS when it is in excess of power. The commonly used ESSs for the purpose include battery energy storage system (BESS), flywheel energy storage system (FESS), and ultracapacitor (UC) [2, 3]. Many studies have reported in literature for frequency regulation in HPS using different

control concepts and algorithms such as PI/PID controller,  $H_\infty$  controllers, and sliding mode controllers [4-7]. To obtain the best possible performance, optimal tuning of the controller parameters is a necessity and as such various evolutionary optimization algorithms tuned control techniques like genetic algorithm (GA) tuned PI/PID control [8], bacterial foraging optimization algorithm (BFOA) and quasi-oppositional harmony search based I/PI [9,10], hybrid BFOA-particle swarm optimization (PSO) based PI control [11], Differential evolution (DE) based PID [12], grey wolf optimization (GWO) and modified GWO tuned PI/PID, fuzzy PID control [13,14,15] have been reported to have been utilized for frequency regulation in different configurations of power systems. The I/PI control and robust decentralized PI-control with time delay have been put forth for mitigation of frequency excursions in a multi-area hydrothermal power network [16,17]. However, owing to nonlinearities and randomness of HPS, the response of I/PI/PID control gets degraded, so, realizing the need for alternative solutions, many researchers have presented frequency regulation studies in power systems using the intelligent control strategies. Fuzzy logic control (FLC) finds its use in frequency regulation study resulting in improved system stability



[18]. Fractional order controllers, owing to their flexibility and ascendancy, have found numerous applications [19-22]. Recently, many evolutionary optimization algorithms such as Chaotic-PSO [23], symbiotic organism search (SOS) [24], modified black hole algorithm (MBHA) [25], artificial bee colony (ABC) [26], and whale optimization algorithm (WOA) [27] have found their use in frequency control applications in coordination with fractional order controllers.

Recently, yet another evolutionary algorithm called SSA is proposed by S. Mirjalili [28] with the potential of use in engineering design problems. The SSA has the advantage of converging rapidly towards optimal value besides possessing the less number of factors to be regulated. This algorithm has found application in frequency regulation vis-à-vis load variations in power system [29].

In light of these observations, this work implements the SSA optimized FOPID control scheme for regulation of frequency under different operating conditions in the HPS. Followed by introduction in section 1, system configuration is described in section 2 and subsequently section 3 presents detailed discussion of FOPID controller. Section 4 describes, with the help of a flowchart, steps involved in implementation of SSA, while section 5 contains discussion on results. Lastly, section 6 concludes the findings.

## 2. HYBRID POWER SYSTEM CONFIGURATION

The proposed HPS, as shown in Fig. 1 and whose parameters are given in table 1, comprises renewable sources-solar, wind- integrated with different ESSs, and DEG. The controller parameters are optimized using SSA with ISE, given by (1), as the objective function [30].

$$ISE = \int_0^{T_{max}} (\Delta f)^2 dt \quad (1)$$

Where,  $\Delta f$  is the frequency deviation of HPS. The ISE is minimized under the following constraints:

$$K_{1min} \leq K_1 \leq K_{1max}$$

$$K_{2min} \leq K_2 \leq K_{2max}$$

$$K_{PImin} \leq K_{PI} \leq K_{PImax}$$

$$K_{DImin} \leq K_{DI} \leq K_{DImax}$$

$$\lambda_{min} \leq \lambda \leq \lambda_{max}$$

$$\mu_{min} \leq \mu \leq \mu_{max}, \text{ where, range of all scaling factors and gains are } [0.1, 2].$$

TABLE 1. GAINS AND TIME CONSTANTS OF VARIOUS SUBSYSTEMS OF HPS

Subsystems	Gains	Time Constants
Wind Turbine Generator (WTG)	$K_{WTG} = 1$	$T_{WTG} = 1.5$
Solar Thermal Power Generation (STPG)	$K_{sol} = 1.8,$ $K_T = 1$	$T_{sol} = 1.8, T_T = 0.3$
Fuel Cell (FC)	$K_{FC} = 0.01$	$T_{FC} = 4$
Aqua Electrolyzer (AE)	$K_{AE} = 0.002$	$T_{AE} = 0.5$
BESS	$K_{BESS} = -0.003$	$T_{BESS} = 0.1$
FESS	$K_{FESS} = -0.01$	$T_{FESS} = 0.1$
UC	$K_{UC} = -0.7$	$T_{UC} = 0.9$
DEG	$K_{DEG} = 0.003$	$T_{DEG} = 2$

The power system can be mathematically expressed using transfer function- as the ratio expressed in (2):

$$G_{sys}(s) = \frac{\Delta f}{\Delta P_e} = \frac{1}{(D+Ms)} \quad (2)$$

$$\Delta P_e = P_L - P_S \quad (3)$$

### 2.1 Brief description of various generating systems

The power outputs from WTG, Solar, DEG, and FC consists of various nonlinearities which in its simplified form can be expressed using first order transfer function, given by (4-7), with associated time constants and gains whose values are given in table 1 [2,30].

$$G_{WTG}(s) = \frac{K_{WTG}}{1+sT_{WTG}} = \frac{\Delta P_{WTG}}{\Delta P_W} \quad (4)$$

$$G_{STPG}(s) = \left( \frac{K_s}{(sT_s+1)} \right) \left( \frac{K_T}{sT_T+1} \right) = \frac{\Delta P_{STPG}}{\Delta P_{sol}} \quad (5)$$

$$G_{FC_k}(s) = \frac{K_{FC}}{(sT_{FC}+1)} = \frac{\Delta P_{FC_k}}{\Delta P_{AE}}, k = 1, 2 \quad (6)$$

$$G_{DEG}(s) = \frac{K_{DEG}}{(sT_{DEG}+1)} = \frac{\Delta P_{DEG}}{\Delta u} \quad (7)$$

### 2.2 Aqua-Electrolyzer

The aqua-electrolyzer, making use of part of the power generated by RES, produces hydrogen for fuel cells. The dynamic behavior of the FC is described by transfer function as in (8) [2], and two FCs use  $(1-K_n)$  of the power generated by solar and wind for feeding to the grid.

$$G_{AE}(s) = \frac{K_{AE}}{(sT_{AE}+1)} = \frac{\Delta P_{AE}}{((\Delta P_{WTG} + \Delta P_{STPG})(1-K_n))} \quad (8)$$

$$K_n = \frac{P_t}{(P_{WTG} + P_{STPG})}, K_n = 0.6 \quad (9)$$

### 2.3 Energy Storage Systems

For load balancing FESS, BESS, and UC are used to either absorb energy from the system when in excess or inject energy into the system when in deficit. These ESSs are introduced in feedback path, independent of

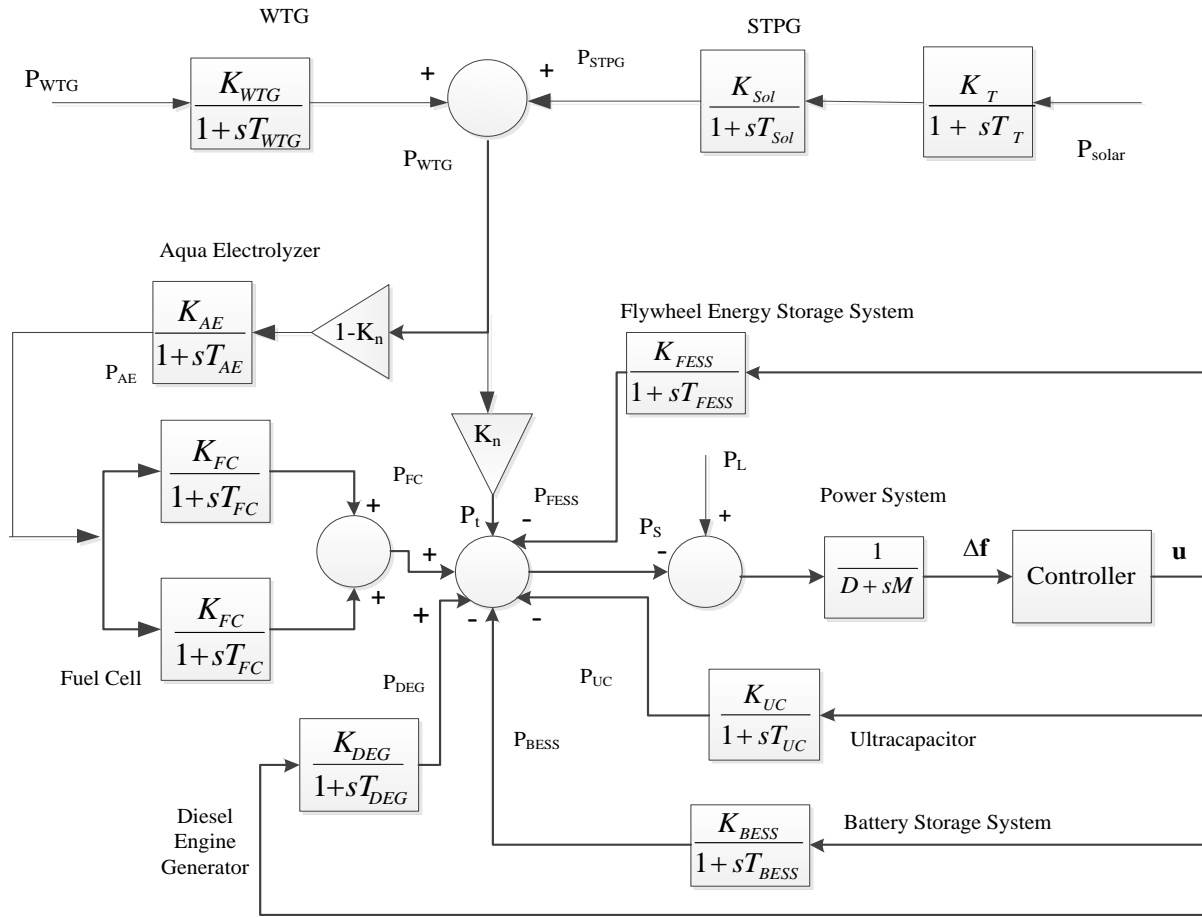


Figure 1. Detailed schematic of the HPS

energy sources and are activated by the FOPPID controller only.

The transfer function representation of these devices is given by (10-12) [2,7].

$$G_{FESS}(s) = \frac{K_{FESS}}{(sT_{FESS}+1)} = \frac{\Delta P_{FESS}}{\Delta u} \quad (10)$$

$$G_{BEES}(s) = \frac{K_{BEES}}{(sT_{BEES}+1)} = \frac{\Delta P_{BEES}}{\Delta u} \quad (11)$$

$$G_{UC}(s) = \frac{K_{UC}}{(sT_{UC}+1)} = \frac{\Delta P_{UC}}{\Delta u} \quad (12)$$

#### 2.4 Provisory models for renewable energy sources

The model of RESs coupled with the load, as described by (13), is obtained using a single template which takes into account the unpredictability associated with output powers of WTG, Solar, and the load [30].

$$P = \left( \frac{\gamma\theta\sqrt{\rho}(1-G(s))+\rho}{\rho} \right) \tau = \varepsilon\tau \quad (13)$$

Where, P signifies the power as available from WTG, solar or load model;  $\gamma$  accounts for unpredictability component of power;  $\rho$  depicts the contribution towards

mean value of power;  $G(s)$  being the mathematical representation, in terms of transfer function, of the low pass filter; and  $\tau$  is the switching signal dependent on time for controlling the variations in mean of output power. In respect of solar power, the various parameters are:  $\gamma \sim U(-1,1), \theta = 0.7, \rho = 2$ ,  $G(s) = \frac{1}{(10^4s+1)}$ ,  $\varphi = 0.1$ , and  $\tau = 1.1111H(t) - 0.5555H(t - 40)$ , wherein  $H(t)$  represents the signal which is called as heaviside step signal. Likewise, variables of (13) for wind power are  $\gamma \sim U(-1,1), \theta = 0.8, \rho = 10$ ,  $G(s) = \frac{1}{(10^4s+1)}$ ,  $\varphi = 1$ , and  $\tau = 0.5H(t) - 0.1H(t - 40)$ . are  $\gamma \sim U(-1,1), \theta = 0.8, \rho = 10$ ,  $G(s) = \frac{1}{(10^4s+1)}$ ,  $\varphi = 1$ , and  $\tau = 0.5H(t) - 0.1H(t - 40)$ .

For load model, variables of (13) are defined as  $\gamma \sim U(-1,1), \theta = 0.8, \rho = 100, \varphi = 1$ ,  $G(s) = \left( \frac{300}{(300s+1)} - \left( \frac{1}{(1800s+1)} \right) \right)$ , and  $\tau = H(t) + \left( \frac{0.8}{\varepsilon} \right) H(t - 80)$ . The power outputs of solar, WTG, and the load model, as obtained by simulating (13) with appropriate parameters, respectively, and also the combined power of



both solar and WTG, ‘P(t)’, are given in fig 2. Due to the stochastic factor built in the model, the sudden changes in the output powers at different time instants i.e. 40 sec. and 80 sec. are visible in the fig 2.

**3. FRACTIONAL ORDER FUZZY PID CONTROLLER**

Recently, wide variety of mathematical techniques is being used to establish models of system by fractional differential equation that can describe better system dynamic characteristics. Fractional calculus is the significant approach with the powers of both differentiation and integration being fractional values [19-22]. There are three well established definitions viz. the Grünwald–Letnikov (GL), Riemann–Liouville (RL), and Caputo, out of which Caputo is frequently employed in automatic control applications and is defined as

$$\alpha D_t^r f_x(t) = \frac{1}{\Gamma(m-r)} \int_a^t D^m f_x(\tau) d\tau, r \in R^+, m \in Z^+ \text{ and } m - 1 \leq r < m \tag{14}$$

Where,  $\alpha^{\text{th}}$  signifies the order of the differ-integral of  $f(t)$ .

The standard mathematical model representation of conventional PID controller using the transfer function approach is as under

$$C(s) = Kp + \left(\frac{K_i}{s}\right) + K_d s \tag{15}$$

Where, the gains:  $K_p, K_i,$  and  $K_d$  correspond to the controller’s proportional, integral, and derivative actions, respectively. Consequently, the generalized model of fractional order PID control is expressed as

$$C(s) = Kp + \left(\frac{K_i}{s^\lambda}\right) + K_d s^\mu \tag{16}$$

Where,  $\lambda,$  and  $\mu$  represent the fractional order parameters both of which if selected equal to 1 will make the controller structure reduce to the conventional PID controller as presented by (15). The fractional order controllers are linear filters and the Oustaloup filters give a good realization of the fractional operators within the typical frequency range ( $\omega_b, \omega_h$ ) (16,17) and order  $N$ . For the proposed controller, the Oustaloup’s filter is considered with order 5 and the frequency range of  $\omega$  [ $10^{-2}, 10^2$ ] rad/sec.

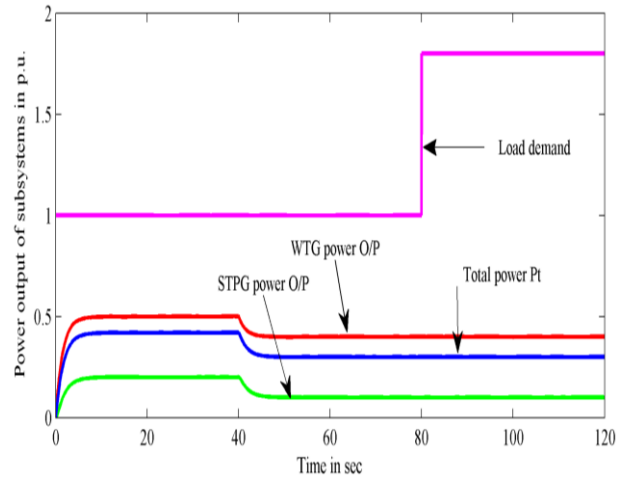


Figure 2. Power output of STPG, WTG, Total generated power P, Load model output

$$G_f(s) = s^\gamma \approx K \prod_{k=-N}^N \frac{s + \omega_k}{s + \omega_k} \tag{17}$$

The proposed controller, as implemented in this study, is FOFPID whose structure is shown in fig 3. This structure combines the advantages of Fuzzy logic and fractional order PID [19] with  $K_1, K_2$  and  $K_{PI}, K_{PD}$  as the input and output weighting factors with  $\lambda, \mu$  as the order of differ-integral. The Fuzzy controller here makes use of three linguistic variables- two inputs and one output- which are further subdivided into five linguistic values each: NL, NS, ZZ, PS, and PL with their respective meanings as negative large, negative small, zero, positive small, and positive large. Mamdani fuzzy inference mechanism serves at the core for drawing inferences whereas, center of gravity is the method employed for defuzzification [18,24,31]. The suitable set of fuzzy rules, as designed, is given in Table 2 while Figure 4 depicts the spread of linguistic terms as represented by suitable membership functions, for input and output variables. The controller parameters are optimally tuned using SSA.

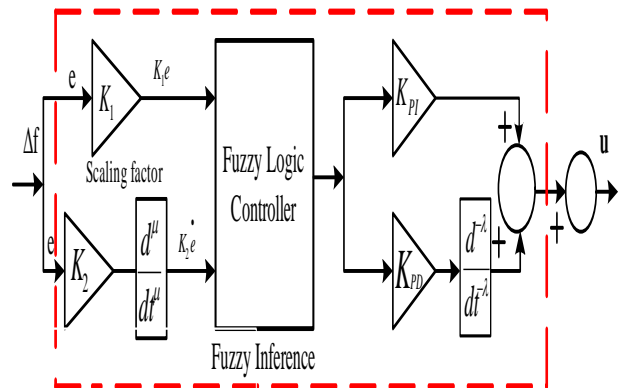


Figure 3. FOFPID control structure

TABLE 2. FUZZY RULE BASE

e \ de/dt	NL	NS	ZZ	PS	PL
PL	ZZ	PM	PL	PS	PL
PS	NM	ZZ	PS	PM	PL
ZZ	NL	NS	ZZ	PS	PL
NS	NL	NM	NS	ZZ	PM
NL	NL	NL	NL	NM	ZZ

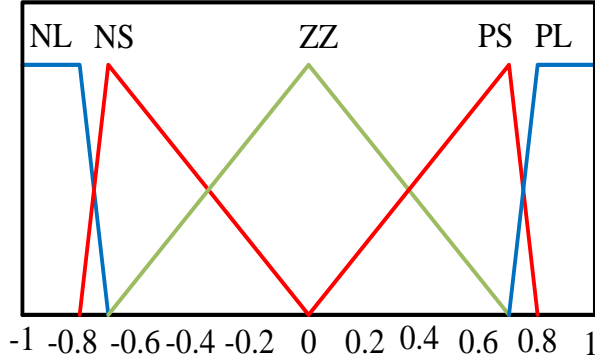


Figure 4. Membership functions for inputs and outputs

**4. OPTIMIZATION TECHNIQUE : SSA**

SSA derives its inspiration from swarming behavior of the salps called salp chains in the deep ocean which is mathematically modeled by Mirjalili [28]. The salp chain or the random population is grouped into two separate clusters and given the names as leader and follower. The position of leader is updated as per (18) w.r.t. food location.

$$y_j^1 = \begin{cases} T_j + a_1(hb_j - lb_j)a_2 + lb_j, & a_3 \geq 0 \\ T_j - a_1(hb_j - lb_j)a_2 + lb_j, & a_3 < 0 \end{cases} \quad (18)$$

Where,  $y_j^1$  and  $T_j$  represent the leader’s position and location of food, respectively, in  $j^{th}$  dimension, whereas,  $hb_j$  and  $lb_j$  signify the upper and lower bounds of the  $j^{th}$  dimension and  $a_1, a_2$  and  $a_3$  are the random numbers. The coefficient  $a_1$  ensures balance between the two processes- exploration and exploitation- and is described as in (19).

$$a_1 = 2e^{-\frac{4s}{S}} \quad (19)$$

Where,  $s$  and  $S$  represent, respectively, the numbers signifying the present and maximum iterations. The follower salp in the chain gets its position updated as per (20).

$$y_j^i = \frac{1}{2}ct^2 + v_0t \quad (20)$$

$i \geq 2$ ,  $y_j^i$  is the position of  $i^{th}$  follower salp in  $j^{th}$  dimension,  $t$  indicates time, whereas, initial speed is indicated by  $v_0$ , and  $c = \frac{v_{final}}{v_0}$  with  $v_{final} = \frac{v - y_0}{t}$ .

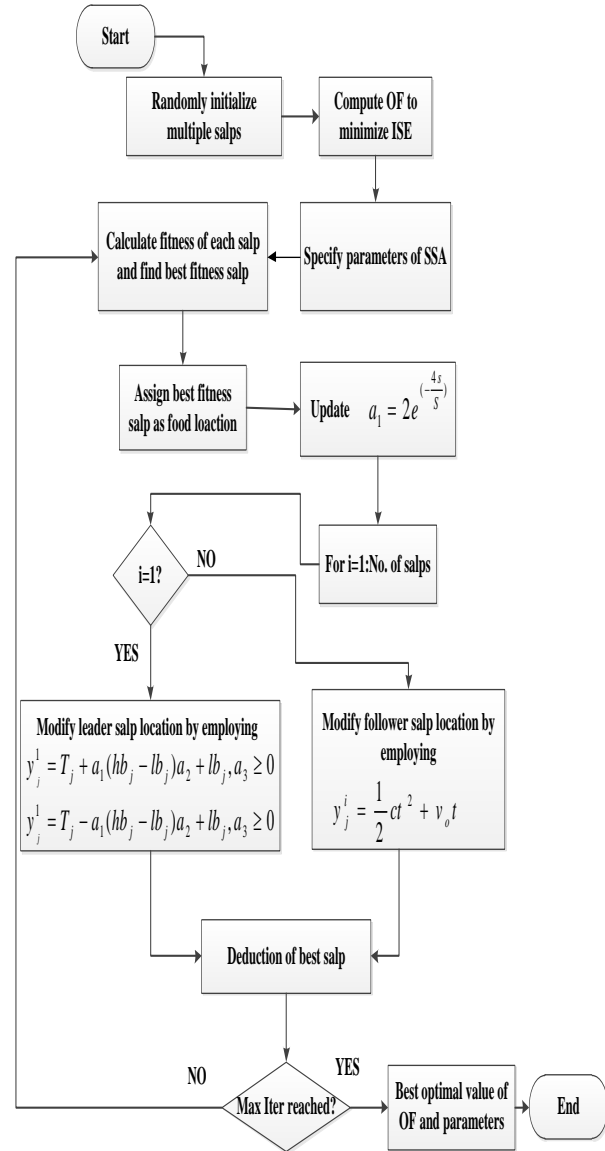


Figure 5. Flow chart for SSA

The iteration count, indicative of the time taken in the optimization process, is expressed as (taking  $v=0$ )

$$y_j^i = 1/2(y_j^i - y_j^{(i-1)}) \quad (21)$$

The algorithmic flow of sequential events in SSA is described in the form of flow chart in Fig. 5.

The salient features and strengths of SSA can be summarized as under:

- i) The  $a_1$  is the significant parameter and decreases with the iteration count.
- ii) SSA is a straightforward and direct algorithm to implement.
- iii) The best salp position is saved which serves as the food location and remains stored even if the whole population deteriorates



## 5. RESULTS AND DISCUSSION

The simulation results, as obtained through various simulation runs on the HPS of Fig 1 for different case studies using MATLAB environment, are described in the following categories:

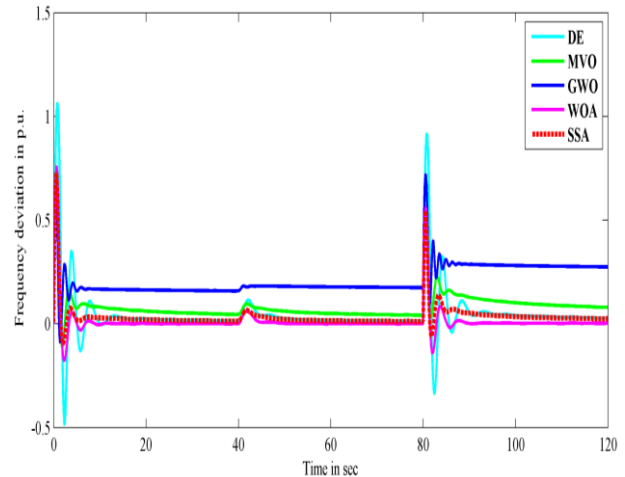
- SSA vis-à-vis other evolutionary algorithms
- Evaluation of FOPID controller against other control methodologies
- Performance evaluation in the backdrop of parametric variations in UC
- Robustness study in the backdrop of disconnection of ESSs, one at a time

### 5.1 SSA vis-à-vis other evolutionary algorithms

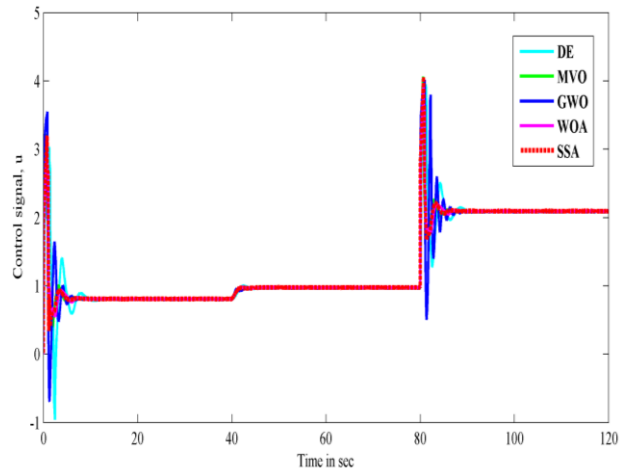
This is just to compare SSA against other evolutionary algorithms with the system given in fig 1 being simulated with varying operating conditions. The controller used is FOPID whose parameters are optimized using SSA, DE, GWO, multiverse optimization (MVO) [32], and WOA algorithms. The results reveal that the objective function (ISE) value is the least with SSA as compared to other algorithms implemented here besides PSO, not implemented here, as well [23]. Table 3 gives the comparative analysis of the quantitative performance of different algorithms in respect of ISE values besides giving the values of FOPID controller gain parameters. The qualitative comparison of performance of various algorithms is given in fig 6 from where it can be brought out that both the frequency deviations and the control signal show less oscillatory response in case of SSA as compared to other algorithms. From table 3 and fig 6, it is amply clear that the SSA outperforms other algorithms.

TABLE 3. COMPARATIVE ANALYSIS OF VARIOUS EVOLUTIONARY ALGORITHMS

Algorit hm	DE	MVO	GWO	WOA	SSA	
<b>ISE</b>	2.3314	0.49787	0.494	0.44814	0.39953	
<b>Controller parameters</b>						
<b>F O P I D</b>	$K_1$	1.5025	1.8888	2	2	2
	$K_2$	0.5102	0.84284	1.5007	1.0388	1.0937
	$K_{PI}$	1.3982	2	2	2	2
	$K_{PD}$	1.9186	2	2	2	2
	$\lambda$	0.8909	0.6393	0.31514	0.9999	0.83461
	$\mu$	0.5060	0.82851	0.18522	0.7748	0.74679



(a)



(b)

Figure 6. (a,b) Frequency deviation and control signal with different optimization algorithms

The output power variations of FC, DEG various ESSs, and the total power output 'P<sub>s</sub>' are presented in fig 7.

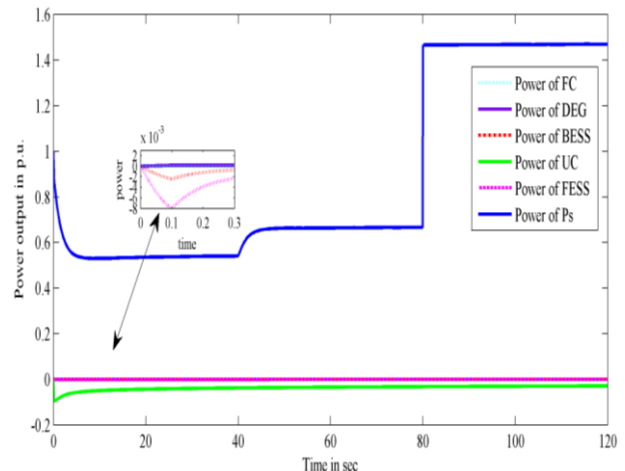


Figure 7. Power output from FC, DEG, BESS, UC, FESS and Ps



5.2 Evaluation of FOFPID controller against other control methodologies

Here, the FOFPID control scheme is evaluated vis-à-vis the other prevalent control schemes like PID/Fuzzy PID under the considering different uncertainties into account. The controller parameters are tuned to SSA algorithm. The uncertainties are introduced at time instants of 40 sec. and 80 sec. As can be inferred from table 4 and fig 8 (a, b), the performance of FOFPID controller turns out to be the best among all three. The FOFPID controller provides effective performance in terms of keeping the frequency deviations low besides response being less oscillatory at the instants of disturbances i.e. at 40 sec. and 80 sec. The control signal variations are also the indicators of the effectiveness of FOFPID controller in respect of smoothness. The FOFPID controller results in value of objective function being the least as is visible in table 4.

TABLE 4. COMPARATIVE MINIMUM VALUES OF ISE AND CONTROLLER PARAMETERS

Controllers	PID	Fuzzy PID	FOFPID
ISE	<b>0.6275</b>	<b>0.79237</b>	<b>0.39953</b>
$K_P, K_I, K_D$	2,2,1.999	---	---
$K_1$	---	1.394	2
$K_2$	---	0.4966	1.0937
$K_{PD}$	---	2	2
$K_{PI}$	---	1.995	2
$\lambda$	---	---	0.83461
$\mu$	---	---	0.74679

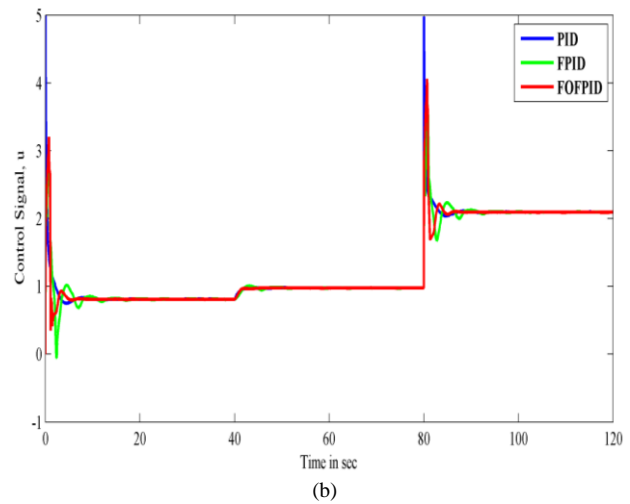
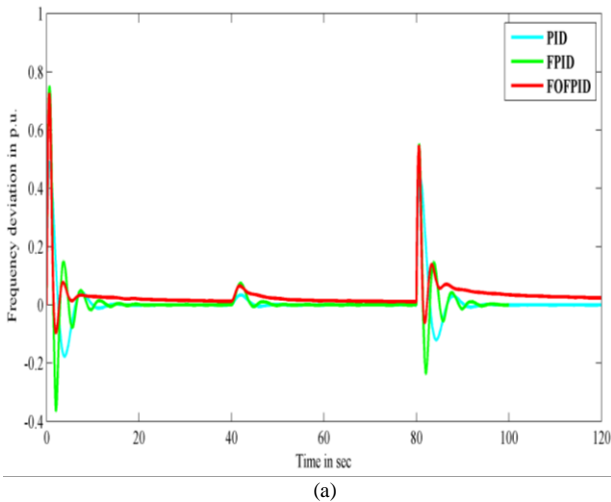


Figure 8. (a,b) Variation of frequency deviation and control signal with different controllers

5.3 Performance evaluation in the backdrop of parametric variations in UC

Under this case study, the performance of controllers, optimally tuned using SSA, is analysed against parametric variations so as to carry out the sensitivity analysis. The UC has the highest power share among all the ESSs. Considering this, the relative evaluation is executed by varying gain and time constant of UC by  $\pm 25\%$  and  $\pm 50\%$ , respectively. The performance measures- frequency and control deviation- for the three controllers with these perturbations is shown in table 5 and fig 9-11 (a,b). It is conspicuous from the results that the SSA optimised FOFPID provides robust and stable control response under extensive variations in the system parameters. For better comprehension of results, the zoomed view of the fig at the time of disturbance is also provided.

TABLE 5. SENSITIVITY ANALYSIS FOR PID/ FPID/ FOFPID FOR UC VARIATIONS

Condition	Performance index ISE for different Controllers		
	PID	FPID	FOFPID
Without Variations	0.6275	0.79237	0.39953
25% decrease	0.8699	0.81517	0.52244
50% decrease	1.6898	1.8154	1.0643
25% increase	0.5150	0.78891	0.37758
50% increase	0.4080	0.47519	0.27733

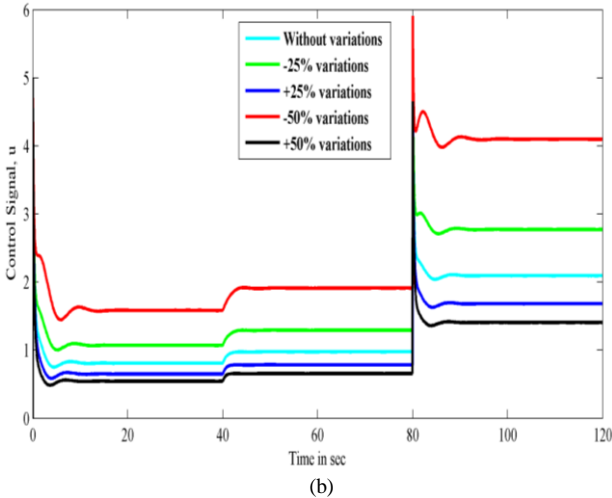
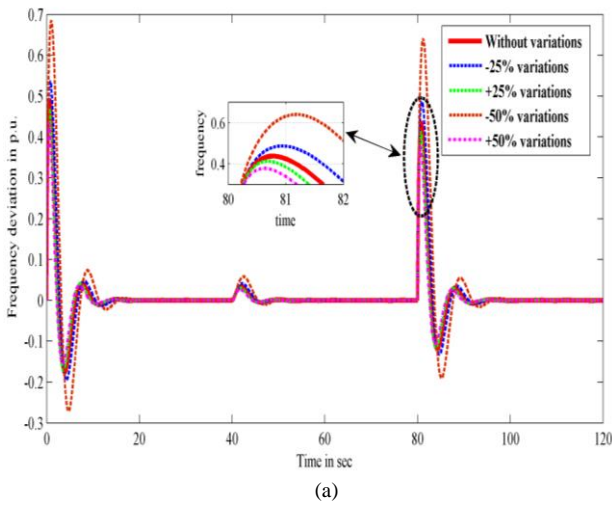


Figure 9. (a,b) Frequency deviation and control signal for PID with variations in gain and time constant of UC

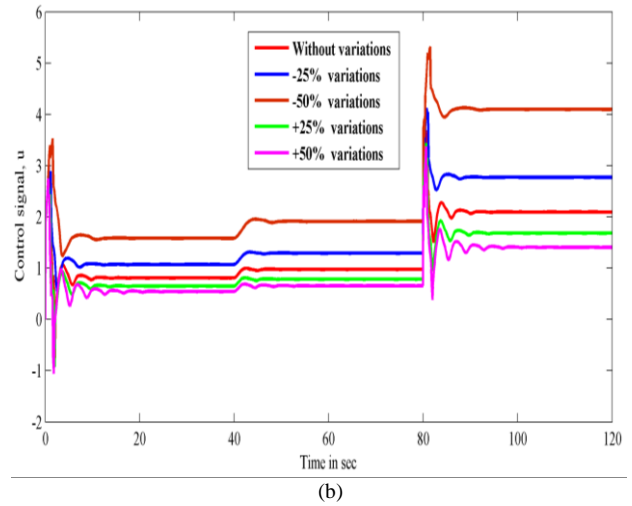
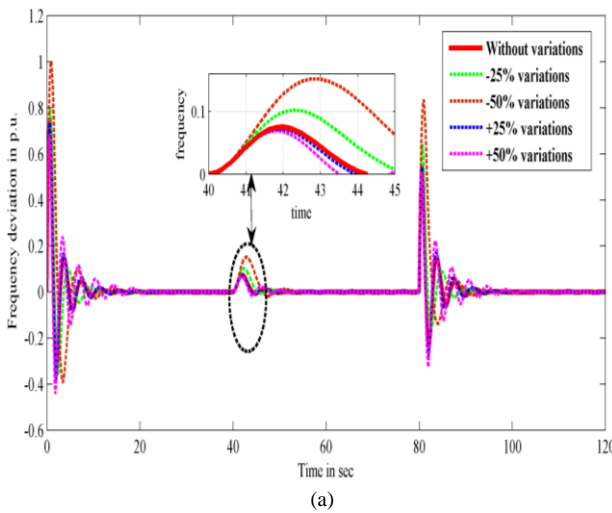


Figure 10. (a,b) Frequency deviation and control signal for FOPID with variations in gain and time constant of UC

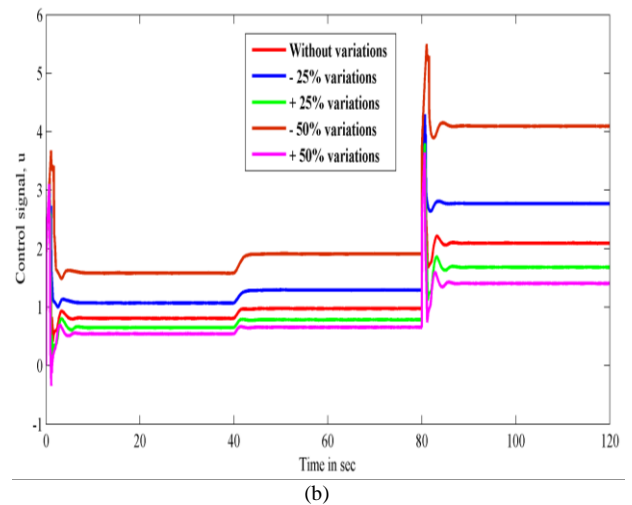
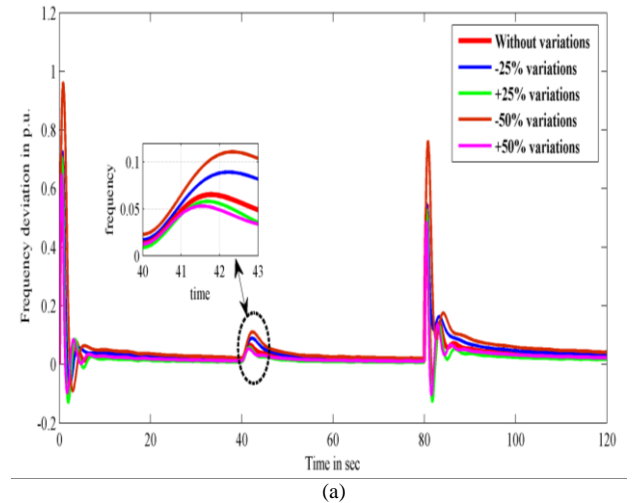


Figure 11. (a,b) Frequency deviation and control signal for FOFPID with variations in gain and time constant of UC

5.4 Robustness study in the backdrop of disconnection of ESSs, one at a time

System is evaluated for its robustness by disconnecting diferent ESSs and DEG, one at a time from the proposed system. For this senario,disconnection of three subsystems i.e. BESS, FESS, DEG is considered and the change in the performance index (ISE) value isobserved which is shown in table 6. The variations in frequency response and control signal output in respect of PID, FPID, and FOFPID is presented in fig 12-14 (a,b) wherefrom the inference can be clearly drawn of the system performance getting highly affected in case of disconnection of FESS as compared to the disconnection of the BESS and DEG, separately. However, the performance of the FOFPID controller remains effective with minimum frequency deviation, even under these disconnections, as compared to other controllers and thereby demonstrating robust and stable behaviour.

TABLE 6. ROBUSTNESS ANALYSIS AGAINST DISCONNECTING SUBSYSTEMS

Controller	Subsystem disconnected	Performance index value
PID	Without disconection	0.62755
	BESS	0.63517
	DEG	0.63069
	FESS	0.65303
FPID	Without disconection	0.79237
	BESS	0.81846
	DEG	0.79981
	FESS	0.88445
FOFPID	Without disconection	0.39953
	BESS	0.5115
	DEG	0.4989
	FESS	0.55062

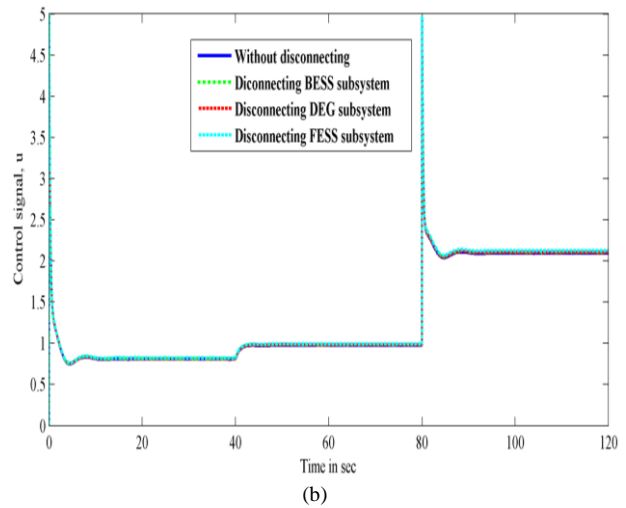
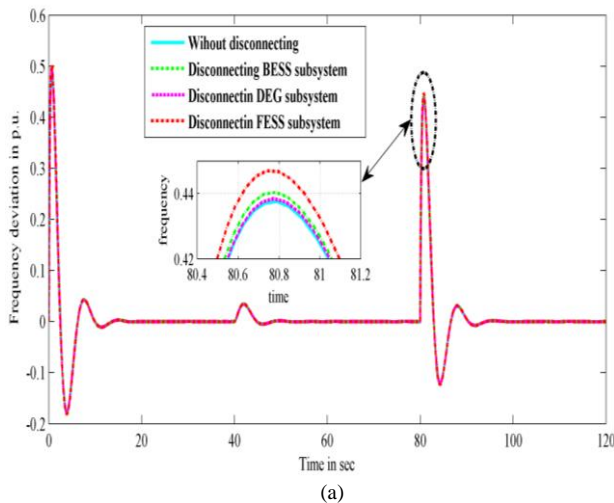


Figure 12. (a, b) Frequency deviation and control output of PID when different subsystems are disconnected

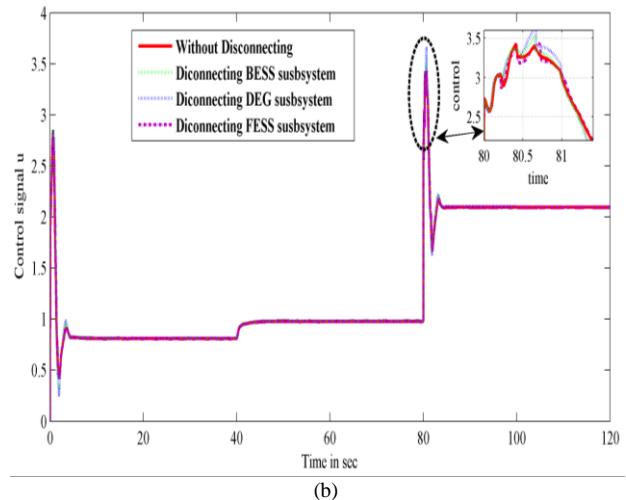
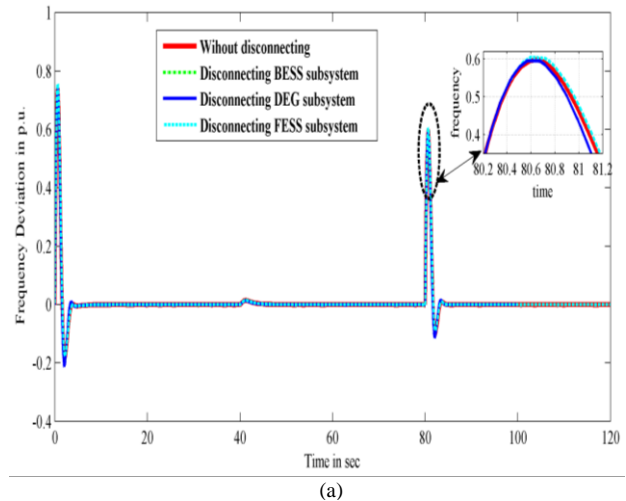


Figure 13. (a, b) Frequency deviation and control output of FPID when different subsystems are disconnected

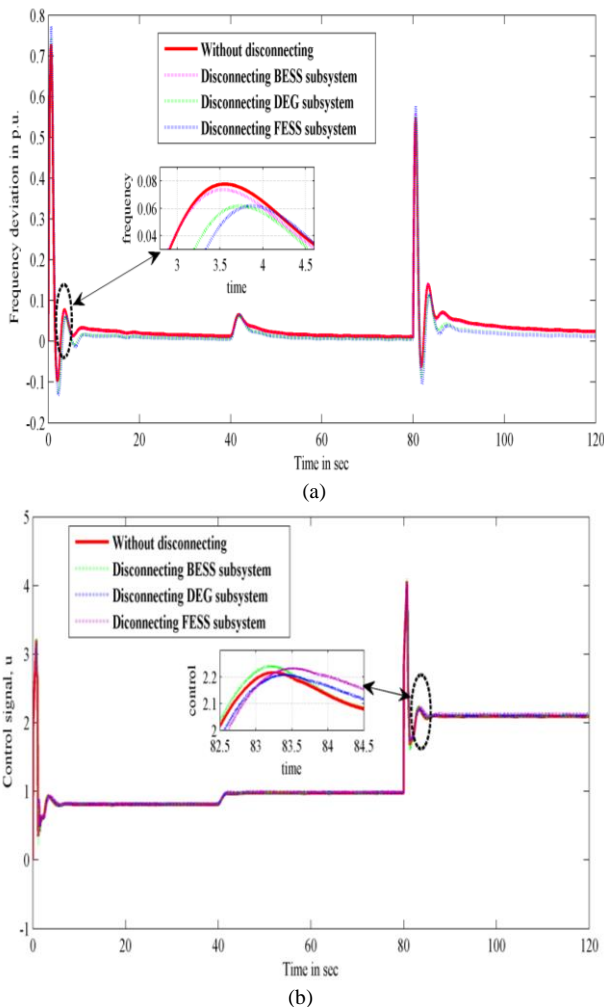


Figure 14. (a, b) Frequency deviation and control output of FOFPID when different subsystems are disconnected

## 6. CONCLUSION

This paper has presented the novel SSA tuned FOFPID control scheme for damping the frequency deviations in a HPS. The novelty lies in the use of SSA, a recently proposed evolutionary optimization algorithm. The proposition proves to be effective even when the operating conditions vary such as load variations, output power variations of solar and wind subsystems, parametric variations in gain and time constant of UC. Also, the supremacy of the SSA has been established against other evolutionary algorithms besides demonstrating the supremacy of the proposed FOFPID control strategy over PID/FPID. The proposed control strategy is proved to be robust and stable under the scenario of any one of the subsystems getting disconnected. Thus, the proposition holds the potential of use in hybrid power systems as an effective control strategy.

## REFERENCES

- [1] M. Uzunoglu, O. C. Onar, M. S. Alam, "Modeling, control and simulation of a PV/FC/UC based hybrid power generation system for stand-alone applications", *Renew Energy*, vol.3, no.34, pp no.509–20, 2009.
- [2] L. Dong-Jing, Li Wang, "Small-signal stability analysis of an autonomous hybrid renewable energy power generation/ energy storage system – Part I: time-domain simulations", *IEEE Trans Electr Power Energy Syst*, vol.1, no.23, pp no.311–20, 2008.
- [3] A. Ahmed Nabil, Masafumi Miyatake, A. K. Al-Othman, "Power fluctuations suppression of stand-alone hybrid generation combining solar photovoltaic/wind turbine and fuel cell systems", *Energy Convers Manage*, vol.10, no. 49, pp no.2711–9, 2008.
- [4] V. Singh, S. Mohanty, N. Kishor, P. Ray, "H-infinity robust load frequency control in hybrid distributed generation systems", *Int J Electr Power Energy Syst*, vol.no.46, pp no. 294–305, 2014.
- [5] S. K. Pandey, N. Kishor, S. R. Mohanty, "Frequency regulation in hybrid power system using iterative proportional–integral–derivative  $H_{\infty}$  controller", *Electr Power Compon Syst*, vol. no. 42, pp no.132–48, 2014.
- [6] K. Vrdoljak, N. Perie, I. Petrove, "Sliding mode based load frequency control in power system", *Electr Power Syst Res*, vol. no. 80, pp no. 514–527, 2010.
- [7] M. Nayeripour, M. Hoseintabar, T. Niknam, "Frequency deviation control by coordination control of FC and double-layer capacitor in an autonomous hybrid renewable energy power generation system", *Renewab. Energy*, vol.6, no.36, pp no.1741–1746, 2011.
- [8] Y. L. Abdel-Magid, M. M. Dawoud, "Optimal AGC tuning with genetic algorithms", *Elect Power Syst Res*, vol.3, no.38, pp no.231–238, 1996.
- [9] E. S. Ali, S. M. Abd-Elazim, "Bacteria foraging optimization algorithm based load frequency controller for interconnected power system", *Int J Elect Power Energy Syst*, vol.3 no.33, pp no.633–638, 2011.
- [10] G. Shankar, V. Mukherjee, "Load frequency control of an autonomous hybrid power system by quasi-oppositional harmony search algorithm", *Electrical Power and Energy Systems*, vol. no. 78, pp no.715–734, 2016.
- [11] S. Panda, B. Mohanty, P. K. Hota, "Hybrid BFOA- PSO algorithm for automatic generation control of linear and nonlinear interconnected power systems", *Applied Soft Comput*, vol.12 no.13, pp no.4718–4730, 2013.
- [12] B. Mohanty, S. Panda, P. K. Hota, "Controller parameters tuning of differential evolution algorithm and its application to load frequency control of multi-source power system", *Int J Electr Power & Energy Syst*, vol. 54, pp no.77–85, 2014.
- [13] D. Guha, P. K. Roy, S. Banerjee, "Load frequency control of interconnected power system using grey wolf optimization", *Swarm Evolution Comput*, vol. no.27, pp no.97–115, 2016.
- [14] M. K. Debnath, T. Jena, S. K. Sanyal, "Frequency control analysis with PID–fuzzy–PID hybrid controller tuned by modified GWO technique", *Int Trans Electr Energ Syst* e12074, vol. 29, no. 10, 2019.

- [15] Y. Sharma, L. C. Saikia, "Automatic generation control of multi-area ST-Thermal power system using Grey Wolf optimizer algorithm based classical controllers", *Electrical power & energy systems*, vol. 73, pp no. 853-862, 2015.
- [16] J. Nanda, A. Mangla, S. Suri, "Some New Findings on Automatic Generation Control of an Interconnected Hydrothermal System with Conventional Controllers", *IEEE Trans on Energy Conv*, vol.1 no.21, pp no.187-194, 2006.
- [17] H. Bevrani, T. Hiyama, "On Load-Frequency Regulation with Time Delays: Design and Real-Time Implementation", *IEEE Trans on Energy Conve*, vol.1 no.24, pp no. 292-300, 2009.
- [18] H. Bevrani, F. Habibi, P. Babahajyani, M. Watanabe, and Y. Mitani, "Intelligent frequency control in an ac microgrid: online PSO-based fuzzy tuning approach", *IEEE transactions on smart grid*, vol. 3, no. 4, pp. 1935-1944, 2012.
- [19] S. Das, *Functional fractional calculus*, Berlin: Springer, 2011.
- [20] C. A. Monje, Y. Q. Chen, B. M. Vinagre, D. Xue, V. Feliu, *Fractional order systems and controls: fundamentals and applications*, London: Springer, 2010.
- [21] H. Bevrani, T. Hiyama, *Intelligent Automatic Generation Control*, CRC Press, 2011.
- [22] I. Podlubny, "Fractional-order systems and  $PI^\lambda D^\mu$  controllers", *IEEE Transactions on Automatic Control*, vol. 44, no.1, pp. 208-214, 1999.
- [23] I. Pan, S. Das, "Fractional order fuzzy control of hybrid power system with renewable generation using chaotic PSO", *ISA Trans*, vol. no.62, pp no. 19-29, 2016.
- [24] Y. Zhou, F. Miao, Q. Luo, "Symbiotic organisms search algorithm for optimal evolutionary controller tuning of fractional fuzzy controller", *Applied Soft Computing J*, vol. no. 77, pp no. 497-508, 2019.
- [25] M. H. Khooban, T. Niknam, M. Shasadeghi, T. Dragicevic, F. Blaabjerg, "Load Frequency Control in Microgrids Based on a Stochastic Noninteger Controller", *IEEE Transactions On Sustainable Energy*, vol. 9, no. 2, pp no. 853-61, 2018.
- [26] A. Abazaria, H. Monsefa, B. Wub, "Coordination strategies of distributed energy resources including FESS, DEG,FC and WTG in load frequency control (LFC) scheme of hybrid isolated micro-grid", *Electrical Power and Energy Systems*, vol. no.109, pp no. 535-547, 2019.
- [27] M. A. Ebrahim, A. Osama, K. M. Kotb, F. Bendary, "Whale inspired algorithm based MPPT controllers for grid-connected solar photovoltaic system", *Energy Procedia*, vol. 162, pp no. 77-86, 2019.
- [28] S. Mirjalili, A. H. Gandomi, S. Z. Mirjalili, S. Saremi, F. Faris, S. M. Mirjalili, "Salp Swarm Algorithm: A bio-inspired optimizer for engineering design problems", *Advances in Engineering Software*, vol.14, pp no.163-191, 2017.
- [29] H. M. Hasaniien, A. A. El-Fergany, "Salp swarm algorithm based optima; load frequency control of hybrid renewable power systems with communication delay and excitation cross coupling effect", *Electrical Power System Research*, vol.119, pp no. 1-8, 2019.
- [30] D. C. Das, A. Roy, N. Sinha, "GA based frequency controller for solar thermal-diesel-wind hybrid energy generation/energy storage system", *Int J Electr Power Energy Syst*, vol.43 no.1, pp no.262-79, 2012.
- [31] Z. W. Woo, H. Y. Chung, J. J. Lin, "A PID type fuzzy controller with self-tuning scaling factors", *Fuzzy Sets and systems*, vol. 115, no. 2, pp no. 321-326, 2000.
- [32] D. Guha, P. K. Roy, S. Banerje, "Multi-verse optimization: a novel method for solution of load frequency control problem in power system", *IET Gen Trans and Dist*, vol.11 no.14, pp no.3601-3611, 2017.



**Shilpam Malik** is pursuing her Ph.D. in the area of load frequency control and modern heuristic optimization techniques in hybrid power system from the National Institute of Technology Kurukshetra, Haryana, India. Her research interests include bio-inspired computing methods, evolutionary optimization algorithms etc. and their applications in power system.



**Sathans Suhag** received his PhD degree in the area of intelligent control and its applications to power systems from the National Institute of Technology Kurukshetra, Haryana, India, in 2012 where, he is currently serving as Professor. His research interests include intelligent control techniques, control issues in hybrid energy systems, evolutionary algorithms and their applications in

power system.